Electronic Supplementary Material (ESI) for Energy & Environmental Science.

Electronic supplementary Information

Highly Efficient ITO-free Organic Solar Cells with the Column-Patterned Microcavity

Jiang Huang [a], Dan Zhao [a], Zifan Dou [a], Qingshan Fan [a], Na Li [a], Shuihai Peng [a], Haoran Liu [b], Yadong Jiang* [a], Junsheng Yu*[a] and Chang-Zhi Li *[b]

[a] State Key Laboratory of Electronic Thin Films and Integrated Devices, School of Optoelectronic Science and Engineering, University of Electronic Science and Technology of China (UESTC), Chengdu 610054, P.R. China
Email: jiangyd@uestc.edu.cn, jsyu@uestc.edu.cn
[b] State Key Laboratory of Silicon Materials, Department of Polymer Science
MOE Key Laboratory of Macromolecular Synthesis and Functionalization and Engineering, Zhejiang University, Hangzhou 310027, P. R. China
Email: czli@zju.edu.cn

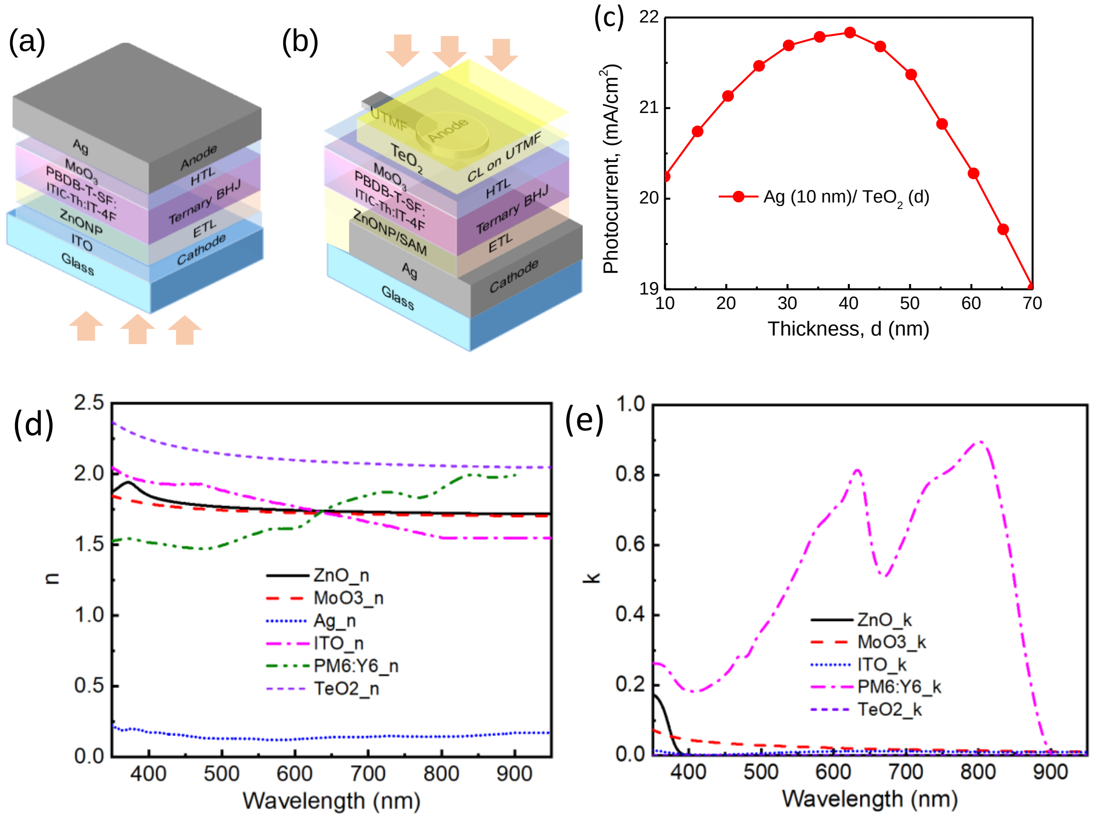

Figure S1. Device architectures of ITO (a) and planar microcavity (MC) OSCs (b) with PBDB-T-SF:ITIC-Th:IT-4F BHJ. (c) the dependence of TeO2 thickness on the photocurrent of planar MC device. (d) and (e) are refractive index n and k of materials used in this work.

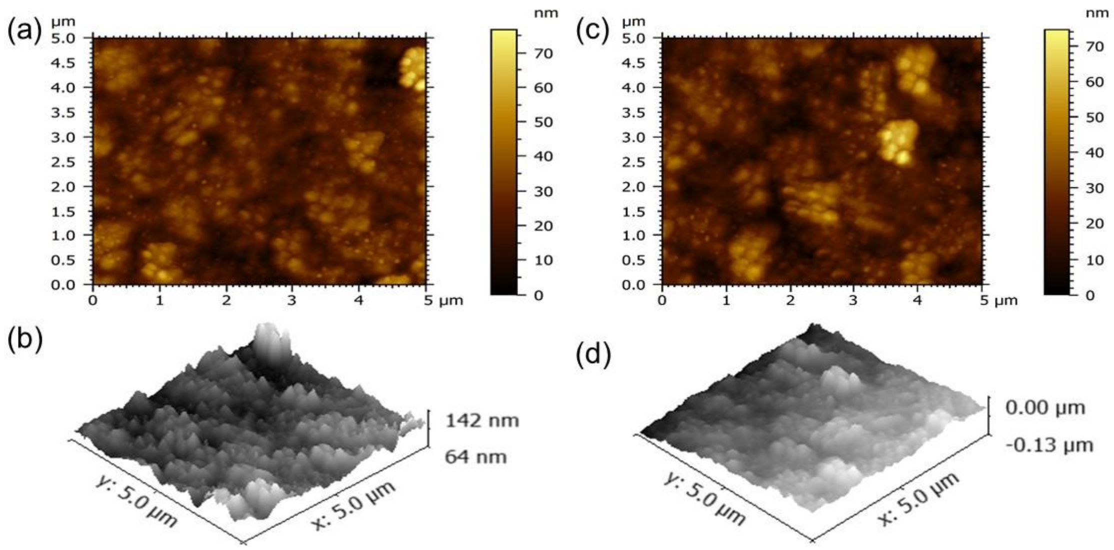

Figure S2. (a, b) AFM images of binary PBDB-T-SF:IT-4F (1:1) and (c, d) ternary PBDB-T-SF:ITIC-Th:IT-4F (1:0.2:0.8) BHJ layers.

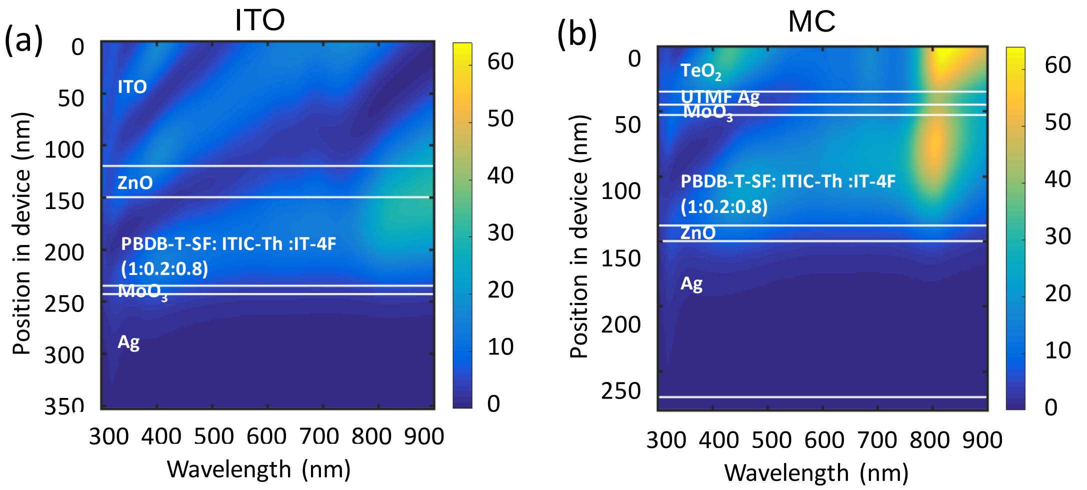

Figure S3. Light distribution of $|E|^2$ in the PBDB-T-SF:ITIC-Th:IT-4F (1:0.2:0.8) BHJ with (a) ITO and (b)microcavity devices.

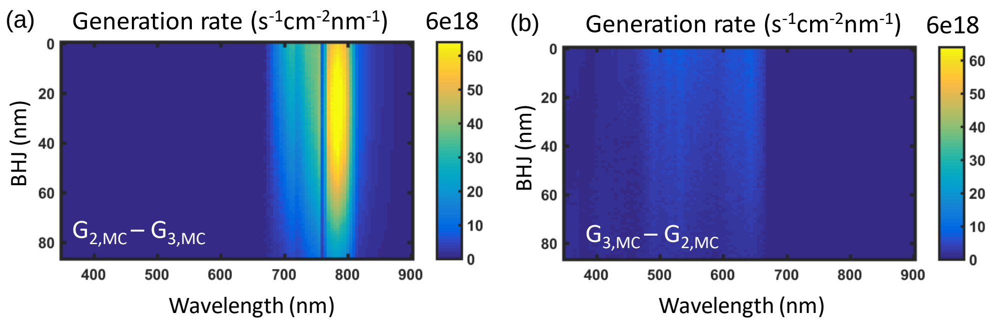

Figure S4. Difference of exciton generation rate (G) (a) $G_{2,MC} - G_{3,MC}$ and (b) $G_{3,MC} - G_{2,MC}$ of planar MC devices. The G_3 is exciton generation rate of ternary device, G_2 is exciton generation rate of binary device.

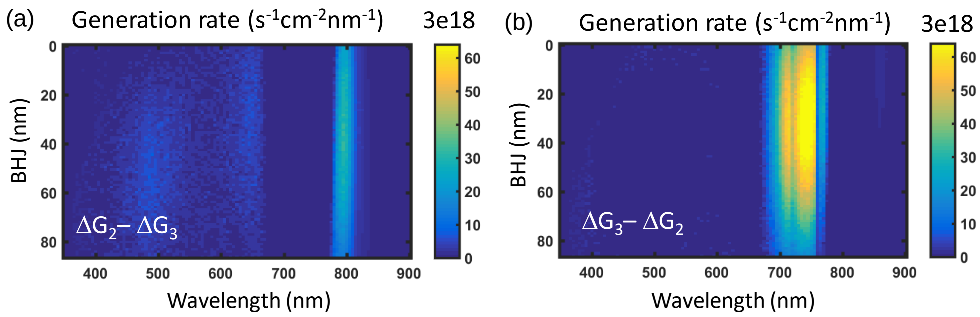

Figure S5. Improvement difference of exciton generation rate (ΔG) (a) ΔG_2-ΔG_3 and (b) ΔG_3-ΔG_2. ΔG_2= $G_{2,MC}$-$G_{2,ITO}$ is the G improvement of binary planar MC and ITO device. ΔG_3=$G_{3,MC}$-$G_{3,ITO}$ is the G improvement of ternary planar MC and ITO device.

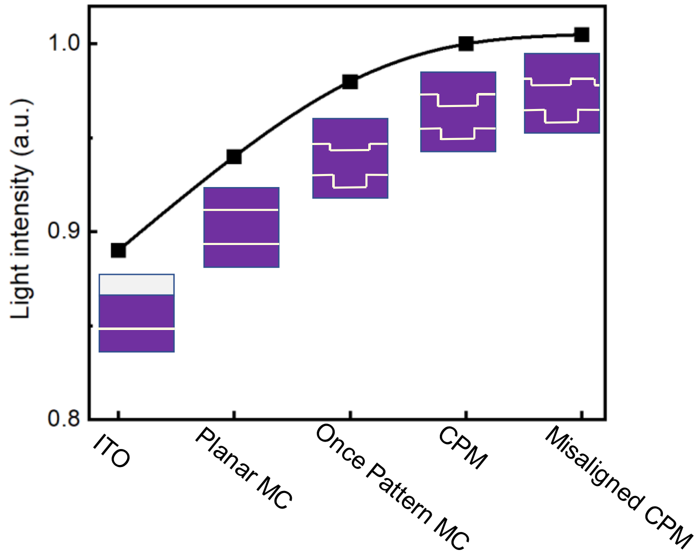

Figure S6. Light intensity comparation of OSCs based on PBDB-T-SF:IT-4F BHJs with different vertical morphology models.

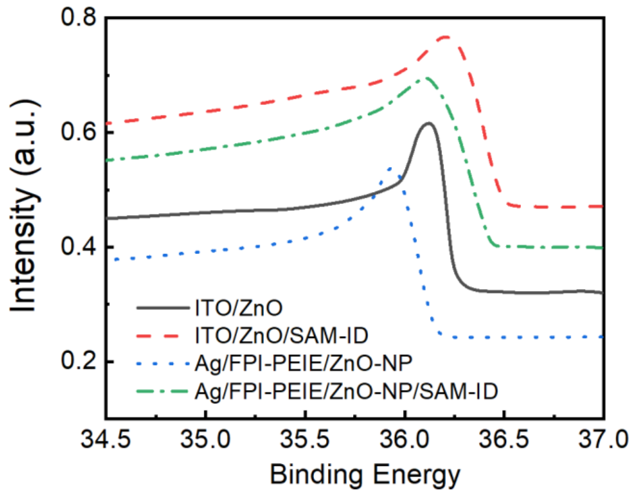

Figure S7. UPS of ZnO and ZnO-NP with and without SAM modification on ITO and Ag/FPI-PEIE electrodes.

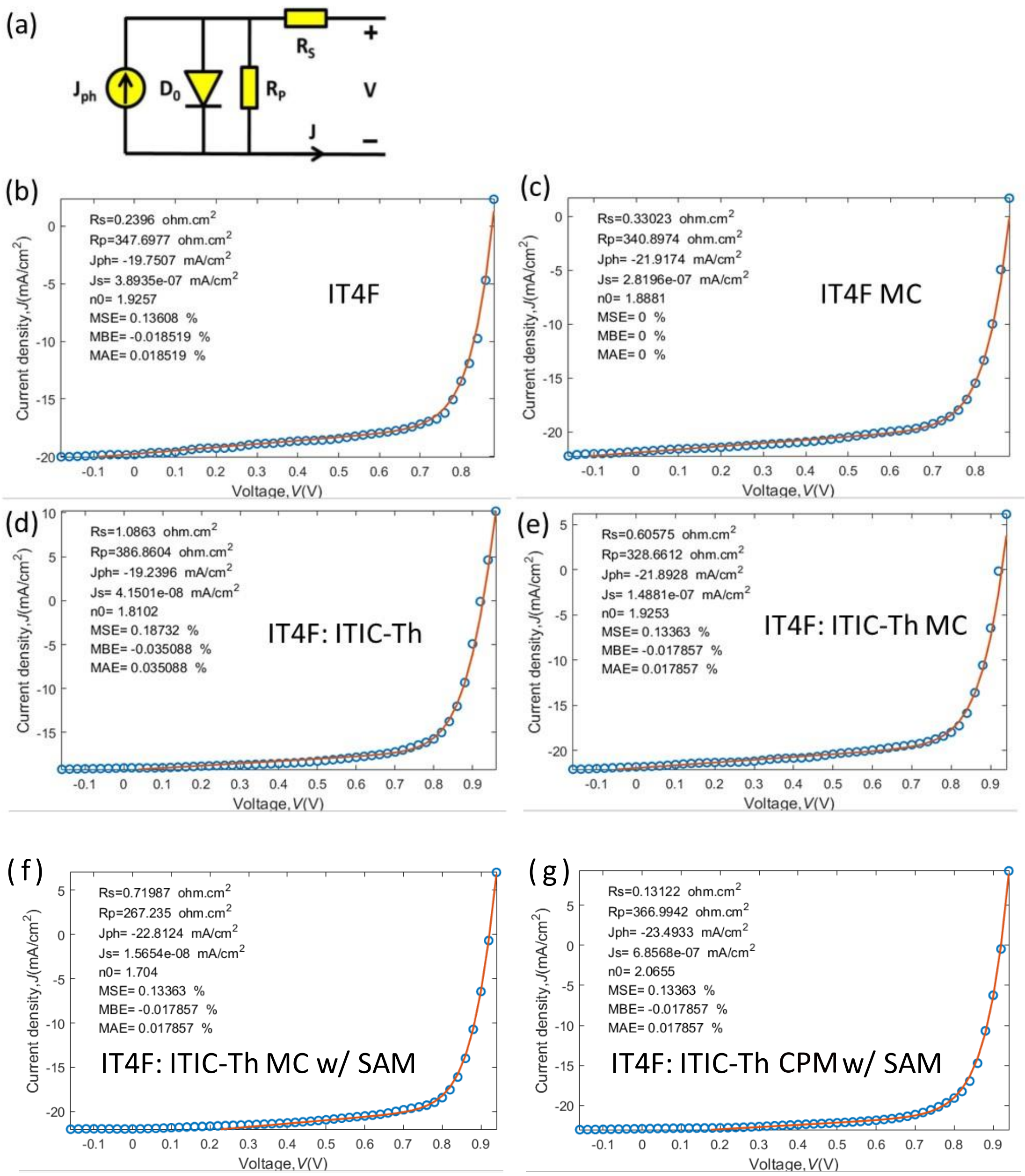

Figure S8. Fittings of J-V curves for extracting equivalent circuit parameters of ITO and microcavity devices.

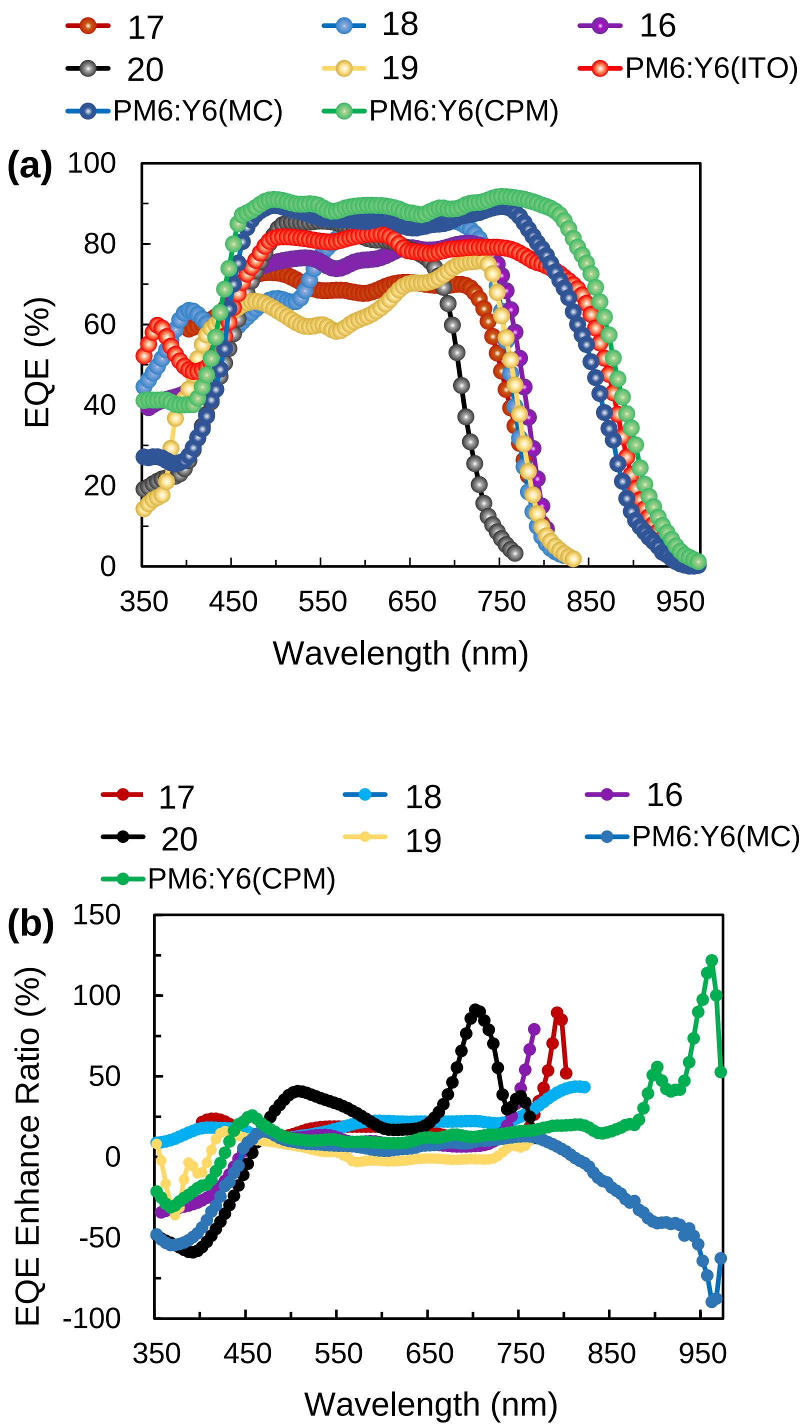

17
18
16
20
19
PM6:Y6(ITO)
PM6:Y6(MC)
PM6:Y6(CPM)
(a)
EQE (%)
100
80
60
40
20
0
350
450
550
650
750
850
950
Wavelength (nm)
17
18
16
20
19
PM6:Y6(MC)
PM6:Y6(CPM)
(b)
EQE Enhance Ratio (%)
150
100
50
0
-50
-100
350
450
550
650
750
850
950
Wavelength (nm)

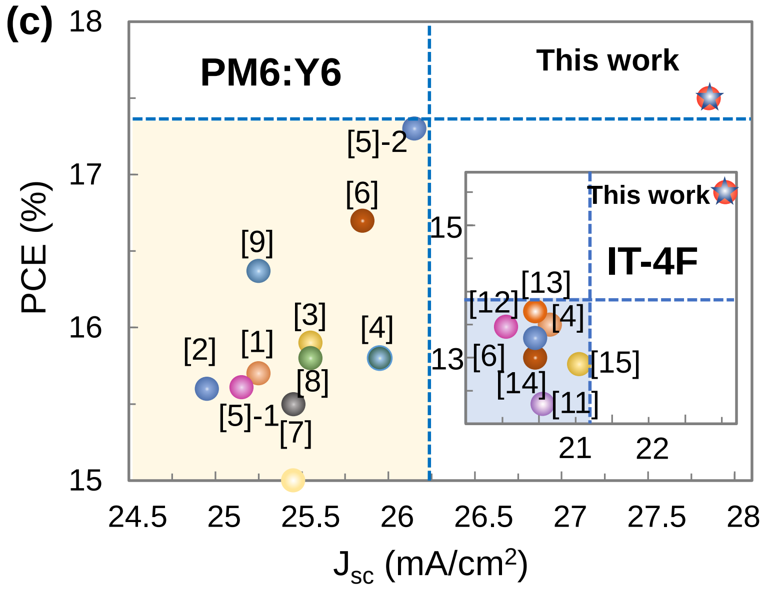

Figure S9. (a) EQE spectra and (b) enhancement ratios (by comparing with the corresponding ITO devices) of OSCs with different optical absorption enhance architectures. (c) The J_{sc} versus PCE comparison of this work and reported OSCs based on PM6:Y6 and IT-4F BHJs.

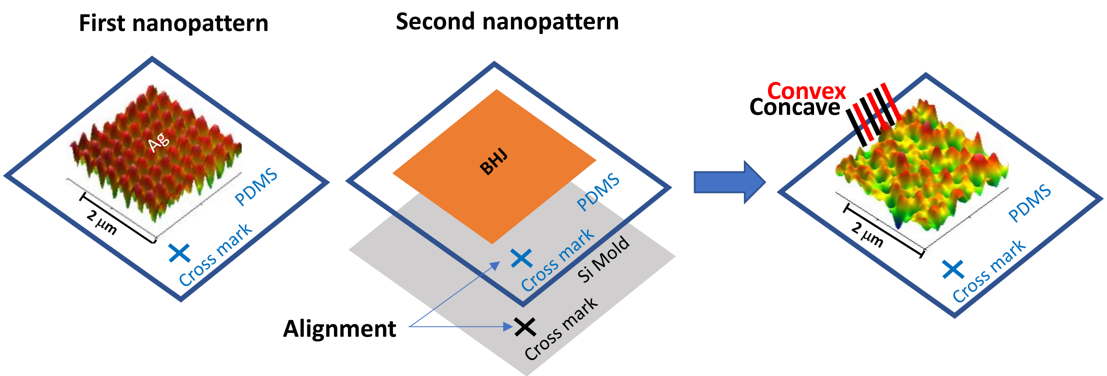

Figure S10. First nanopattern on PDMS templet film and second nanopattern on BHJ film by aligning the cross marks on PDMS and Si mold.

Table S1. The work function and contact angle characteristics of ITO/ZnO, ITO/ZnO/SAM-ID, Ag/FPI-PEIE/ZnO-NP, Ag/FPI-PEIE/ZnO-NP/SAM-ID films.

Film	Work function (eV)	Contact angle (°)
ITO/ZnO	3.75	54.9
ITO/ZnO/SAM-ID	3.48	75.8
Ag/FPI-PEIE/ZnO-NP	3.86	49.3
Ag/FPI-PEIE/ZnO-NP/SAM-ID	3.52	72.5

Table S2. Photovoltaic parameters of OSCs with an ITO configuration and microcavity configuration.

BHJ of OSC (86 ± 3 nm)	J_0 (mA/cm^2)	J_s (mA/cm^2)	n	R_s (Ω·cm^2)	R_p (Ω·cm^2)
PBDB-T-SF:IT-4F (1:1, ITO)[a]	19.75	3.89×10^{-7}	1.93	0.23	347
PBDB-T-SF:IT-4F (1:1, planar MC)[a]	21.92	2.82×10^{-7}	1.89	0.33	340
PBDB-T-SF:ITIC-Th:IT-4F (1:0.2:0.8, ITO)	19.24	4.15×10^{-8}	1.81	1.08	386
PBDB-T-SF:ITIC-Th:IT-4F (1:0.2:0.8, planar MC)	21.89	1.49×10^{-7}	1.93	0.61	328
PBDB-T-SF:ITIC-Th:IT-4F (1:0.2:0.8, planar MC w/ SAM)	22.81	1.56×10^{-8}	1.70	0.72	267
PBDB-T-SF:ITIC-Th:IT-4F (1:0.2:0.8, CPM w/ SAM)	23.49	6.86×10^{-7}	2.07	0.13	367

Table S3. Photovoltaic parameters of OSCs with an ITO configuration and microcavity configuration.

Structure of OSC	V_{oc} (V)	J_{sc} (mA/cm^2)	*FF* (%)	PCE (%)$^{a)}$	*Ref*
PM6:Y6 (ITO)	0.85	24.9	73.7	15.5	This work
PM6:Y6 (CPM w/ SAM)	0.85	27.8	74.5	17.5	This work
PM6:Y6	0.82	25.2	76.1	15.7	[1]
PM6:Y6	0.83	24.9	75.3	15.6	[2]
PM6:Y6	0.84	25.5	74.0	15.9	[3]
PM6:Y6 (WS_2)	0.84	25.9	73.0	15.8	[4]
PM6:Y6:$PC_{71}BM$ (WS_2)	0.84	26.0	78.0	17.0	[4]
PM6:Y6 (CN)	0.844	25.1	73.66	15.61	[5]
PM6:Y6 (GCL)	0.84	26.09	79.05	17.32	[5]
PM6:Y6 (SD)	0.844	25.8	76.7	16.7	[6]
PM6:Y6	0.839	25.37	73.0	15.5	[7]
PM6:Y6	0.86	25.5	72.0	15.8	[8]
PM6:Y6	0.84	25.19	77.3	16.37	[9]
AgNWs/PBDB-T-2F:Y6	0.83	25.4	71.0	15.03	[10]
PBDB-T-SF:IT-4F:	0.87	19.8	71.9	12.4	This work
PBDB-T-SF:ITIC-Th:IT-4F (1:0.2:0.8, CPM w/ SAM)	0.93	22.9	72.7	15.5	This work
PBDB-T-SF:IT-4F (WS_2)	0.88	20.6	74.0	13.5	[4]
IT-4F (SD)	0.867	20.4	75.4	13.3	[6]
AgNWs/PBDB-T-2F:IT-4F	0.82	21.0	75.0	12.9	[10]
PBDB-T-2F:IT-4F	0.82	20.5	73.0	12.3	[11]
PBDB-T-2Cl:IT-4F	0.88	19.9	76.4	13.47	[12]
PBDB-TF:IT-4F	0.87	20.4	77.0	13.7	[13]
PM6:IT-4F	0.86	20.4	74.0	13.0	[14]

References:

[1] J. Yuan, Y. Zhang, L. Zhou, G. Zhang, H.-L. Yip, T.-K. Lau, X. Lu, C. Zhu, H. Peng, P. A. Johnson, M. Leclerc, Y. Cao, J. Ulanski, Y. Li and Y. Zou, Joule, 2019, 3, 1140-1151.

[2] Y. Cui, H. Yao, J. Zhang, T. Zhang, Y. Wang, L. Hong, K. Xian, B. Xu, S. Zhang, J. Peng, Z. Wei, F. Gao and J. Hou, Nat Commun, 2019, 10, 2515.

[3] J. Song, C. Li, L. Zhu, J. Guo, J. Xu, X. Zhang, K. Weng, K. Zhang, J. Min, X. Hao, Y. Zhang, F. Liu and Y. Sun, Advanced Materials, 2019, 31, 1905645.

[4] Y. Lin, B. Adilbekova, Y. Firdaus, E. Yengel, H. Faber, M. Sajjad, X. Zheng, E. Yarali, A. Seitkhan, O. M. Bakr, A. El-Labban, U. Schwingenschlögl, V. Tung, I. McCulloch, F. Laquai and T. D. Anthopoulos, Advanced Materials, 2019, 31, 1902965.

[5] L. Liu, Y. Kan, K. Gao, J. Wang, M. Zhao, H. Chen, C. Zhao, T. Jiu, A.-K.-Y. Jen and Y. Li, Advanced Materials, 2020, 32, 1907604.

[6] H. Fu, W. Gao, Y. Li, F. Lin, X. Wu, J. H. Son, J. Luo, H. Y. Woo, Z. Zhu and A. K.-Y. Jen, Small Methods, n/a, 2000687.

[7] R. Ma, T. Liu, Z. Luo, Q. Guo, Y. Xiao, Y. Chen, X. Li, S. Luo, X. Lu, M. Zhang, Y. Li and H. Yan, Science China Chemistry, 2020, 63, 325-330.

[8] J. Wu, G. Li, J. Fang, X. Guo, L. Zhu, B. Guo, Y. Wang, G. Zhang, L. Arunagiri, F. Liu, H. Yan, M. Zhang and Y. Li, Nature Communications, 2020, 11, 4612.

[9] Z. Luo, R. Ma, T. Liu, J. Yu, Y. Xiao, R. Sun, G. Xie, J. Yuan, Y. Chen, K. Chen, G. Chai, H. Sun, J. Min, J. Zhang, Y. Zou, C. Yang, X. Lu, F. Gao and H. Yan, Joule, 2020, 4, 1236-1247.

[10] F. Qin, W. Wang, L. Sun, X. Jiang, L. Hu, S. Xiong, T. Liu, X. Dong, J. Li, Y. Jiang, J. Hou, K. Fukuda, T. Someya and Y. Zhou, Nature Communications, 2020, 11, 4508.

[11] X. Dong, P. Shi, L. Sun, J. Li, F. Qin, S. Xiong, T. Liu, X. Jiang and Y. Zhou, Journal of Materials Chemistry A, 2019, 7, 1989-1995.

[12] R. Ma, Y. Chen, T. Liu, Y. Xiao, Z. Luo, M. Zhang, S. Luo, X. Lu, G. Zhang, Y. Li, H. Yan and K. Chen, Journal of Materials Chemistry C, 2020, 8, 909-915.

[13] W. Li, L. Ye, S. Li, H. Yao, H. Ade and J. Hou, Advanced Materials, 2018, 30, 1707170.

[14] J. Wan, L. Zhang, Q. He, S. Liu, B. Huang, L. Hu, W. Zhou and Y. Chen, Advanced Functional Materials, 2020, 30, 1909760.

[15] Z. Zhang, H. Wang, J. Yu, R. Sun, J. Xu, L. Yang, R. Geng, J. Cao, F. Du, J. Min, F. Liu and W. Tang, Chemistry of Materials, 2020, 32, 1297-1307.

[16] J. Huang, C. Z. Li, C. C. Chueh, S. Q. Liu, J. S. Yu and A. K. Y. Jen, Advanced

Energy Materials, 2015, 5, 3599-3606(3598).
[17] S. Jeong, C. Cho, H. Kang, K.-H. Kim, Y. Yuk, J. Y. Park, B. J. Kim and J.-Y. Lee, ACS Nano, 2015, 9, 2773-2782.
[18] J.-D. Chen, C. Cui, Y.-Q. Li, L. Zhou, Q.-D. Ou, C. Li, Y. Li and J.-X. Tang, Advanced Materials, 2015, 27, 1035-1041.
[19] W. Shen, G. Zhao, X. Zhang, F. Bu, J. Yun and J. Tang, Nanomaterials, 2020, 10, 944.
[20] K. Yao, X.-K. Xin, C.-C. Chueh, K.-S. Chen, Y.-X. Xu and A. K.-Y. Jen, Advanced Functional Materials, 2015, 25, 567-574.